

IR absorption spectroscopy of carbon dots from citric acid and ethylenediamine: the relationship between their photoluminescence and structure

© A.M. Vervalde¹, K.A. Laptinskiy², M.Yu. Khmeleva¹, T.A. Dolenko¹

¹ Department of Physics, Moscow State University,
119991 Moscow, Russia

² Skobeltsyn Institute of Nuclear Physics,
119991 Moscow, Russia

e-mail: alexey.vervald@physics.msu.ru

Received December 01, 2023

Revised January 11, 2024

Accepted March 05, 2024

In this study, the change in the structure of carbon dots from ethylenediamine and citric acid during their hydrothermal synthesis was studied and the relationship between the structure of nanoparticles and the intensity of their photoluminescence was revealed. For this purpose, a series of carbon dots was synthesized with a precursor ratio of ethylenediamine: citric acid of 2:1 at a temperature of 140 °C and changing the synthesis time from 0.5 to 6 h. Based on the data of IR absorption spectroscopy, photoluminescence spectroscopy and optical absorption spectroscopy, three stages were identified in the synthesis: a chemical reaction at the stage of mixing precursors, the synthesis of highly efficient molecular luminophores when the synthesis time reaches 1 h, carbonization of molecules and the formation of a copolymer framework of carbon dots when the time of synthesis reaches 3 h. It has been established that the formation of a high quantum yield of photoluminescence of carbon dots occurs mainly at the second stage of synthesis.

Keywords: carbon dots, photoluminescence, quantum yield, IR absorption, structure-properties.

DOI: 10.61011/EOS.2024.03.58740.24-24

Introduction

Carbon dots (CDs) feature bright photoluminescence (PL), high chemical stability, and low toxicity, which makes them promising candidates for various biological and optoelectronic applications [1–4]. The applicability of CDs depends largely on the specific features of their PL: intensity and spectral characteristics of emission and their dependence on (or independence of) the properties of a medium and surrounding molecules [1–3,5–7]. The properties of CD PL, in turn, depend significantly and directly on the specifics of nanoparticle synthesis [1,2].

The hydrothermal method is one of the best CD synthesis techniques: it is simple (various protocols of one-pot synthesis are known), cost-effective, and scalable [8–11]. The properties of synthesized CDs may be adjusted by changing the type of CD precursors and their ratio or the process parameters (time and temperature) [2,12]. CDs synthesized this way normally feature a broad luminescence spectrum with a FWHM exceeding 50 nm. Its maximum under excitation by ultraviolet light may fall anywhere from the violet (415 nm [13]) region to the green one (525 nm [14]) and undergoes a redshift right up to 600 nm when the excitation wavelength increases [13,15]. The quantum yield (QY) of this luminescence normally varies from several percent to several tens of percent and, in certain rare cases, reaches ~ 100% [2,16].

A combination of citric acid (CA) and ethylenediamine (EDA) is one of the widely used sets of precursors for hydrothermal CD synthesis. CDs synthesized from these precursors feature intense PL in the blue region with a luminescence QY that, at certain synthesis parameters, exceeds the PL QY of almost any other CDs and may reach 90% [2,16–18]. The results reported in [18] demonstrate that the luminescence QY of these CDs depends on the temperature and time of nanoparticle synthesis, which were varied within the ranges of 140–200 °C and 1–24 h. However, the exact mechanisms of formation of CD PL and the physical basis of the mentioned dependence still remain obscure.

It has been suggested in [19–21] that this luminescence has a molecular mechanism. Presumably, PL of CDs synthesized from CA and EDA is induced by individual molecular luminophores (citrazinic acid derivatives attached to the carbon framework of CDs). The authors of [20] have analyzed solid-state nuclear magnetic resonance data for CDs produced from a 1:1 CA:EDA mixture and suggested that this luminophore is 5-oxo-1,2,3,5-tetrahydroimidazo[1,2-a]pyridine-7-carboxylic acid (IPCA). Unfortunately, the specific stage of synthesis at which molecular CD luminophores form remains undetermined, and the general nature of variation of the CD structure upon a change in temperature or time of synthesis has not been characterized yet.

In the present study, the changes in PL of CDs synthesized hydrothermally from a 2:1 mixture of EDA and CA at a temperature of 140 °C are examined with the synthesis time varying from 0.5 to 6 h in 0.5 or 1 h increments. The changes in CD structure are analyzed via FTIR spectroscopy, while the optical properties of CDs are studied using PL spectroscopy and optical absorption spectroscopy.

Materials and methods

Citric acid (monohydrate, AR grade, produced by Ruskhim) and ethylenediamine (high-purity, produced by JSC „EKOS-1“) were used as CD precursors. Bidistilled deionized water with a conductivity of 0.055 $\mu\text{S}/\text{cm}$, which was produced using a Millipore Milli-Q purification system, served as a solvent in all experiments.

CDs were synthesized hydrothermally. All CDs were produced from one and the same aqueous solution of a mixture of precursors: 6.7 mL of 0.2 M ethylenediamine were mixed with 10.53 g of 0.1 M citric acid and 487.5 mL of water. Teflon flasks containing this solution were introduced into steel autoclaves, which were then put into a Sputnik (Russia) muffle furnace, held there for 30 min (or 1–6 h with increments of 1 h) at a temperature of 140 °C, and allowed to cool gradually to room temperature. Seven CD solutions synthesized this way were filtered through a membrane filter with a pore size of 0.22 μm in order to remove the coarse particle fraction. The concentration of CDs in synthesized solutions was on the order of 25 g/L.

The pH values of synthesized CD samples measured with an Akvilon I-500 pH meter were 7.6–7.8 (without dilution) and 6.5–6.7 (after dilution by a factor of 4001 for optical measurements; see below). The characteristic zeta potential of CDs synthesized from CA and EDA was on the order of –15 mV, and their hydrodynamic diameter in an aqueous solution was 20 nm, which is 2–3 times greater than the size of individual nanoparticles (6–11 nm) determined by electron microscopy [7]. In what follows, samples are designated in accordance with the synthesis time: CD X h.

PL spectra of aqueous CD solutions were recorded with a Shimadzu RF-6000 spectrofluorimeter, and optical density spectra were measured using a Shimadzu UV-1800 spectrophotometer.

The QY of CD PL in aqueous solutions was determined by the reference dye method [22] as

$$Q = Q_r \frac{OD_r}{OD} \frac{I}{I_r} \left(\frac{n}{n_r} \right)^2,$$

where Q is the QY of CD PL, OD is the optical density, I is the integral PL intensity, and n is the refraction index of the medium; all parameters were determined at wavelength $\lambda_{\text{ex}} = 350$ nm. Index „r“ denotes the corresponding parameters of the reference dye (quinine sulphate in a 0.05 M aqueous solution of sulphuric acid H_2SO_4). The value of

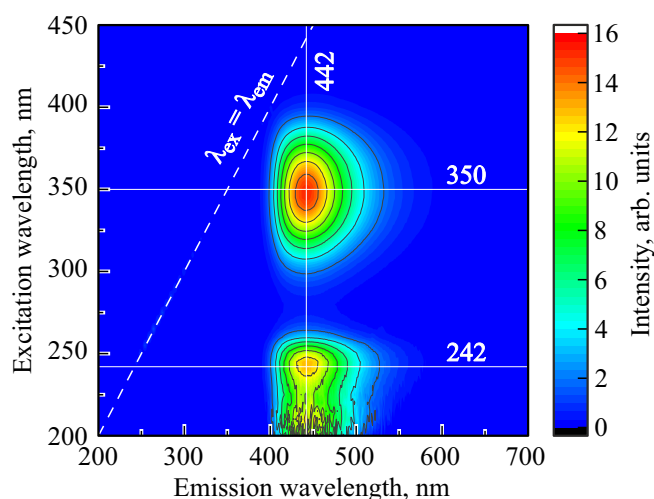


Figure 1. PL excitation/emission maps for an aqueous solution of CD 3 h diluted by a factor of 4001.

58% determined for a wavelength of 350 nm was used as Q_r [22].

IR absorption spectra of samples were recorded with a Bruker INVENIO R FTIR spectrometer. In these measurements, a CD solution droplet was deposited onto the diamond crystal of a frustrated total internal reflection (FTIR) accessory and dried under a steady stream of room air for 10–15 min.

Results and discussion

CD PL

PL excitation/emission maps for aqueous solutions of all the synthesized CDs (Fig. 1 presents such a map for a solution of CD 3 h as an example) are similar and feature two isolated fluorescence centers with maxima around $\lambda_{\text{ex}}/\lambda_{\text{em}} = 350/442$ and $242/442$ nm/nm. These fluorescence maxima correspond to two separate bands in optical absorption spectra with maxima around the same wavelengths of 242 and 350 nm (Fig. 2, a), which are induced by $\pi-\pi^*$ electronic transitions of C=C and/or C-N bonds and $n-\pi^*$ transitions of C=O, C-N, and/or C-OH bonds in sp^3 domains, respectively [23]. Notably, the PL emission spectra measured under excitation at the two indicated wavelengths differ in intensity only. This fact suggests that both PL maxima correspond to one emission center that may be excited following two different energy transition diagrams.

The optical density of most samples at PL excitation wavelength $\lambda_{\text{ex}} = 350$ nm was significantly higher than 4. Thus, in order to perform a correct comparison of PL of different CD samples, these solutions were diluted so that their optical density at λ_{ex} was on the order of 0.1 (this value was chosen so as to suppress the internal filter effect). The initial solution in the series (sample CD 0.5 h) was

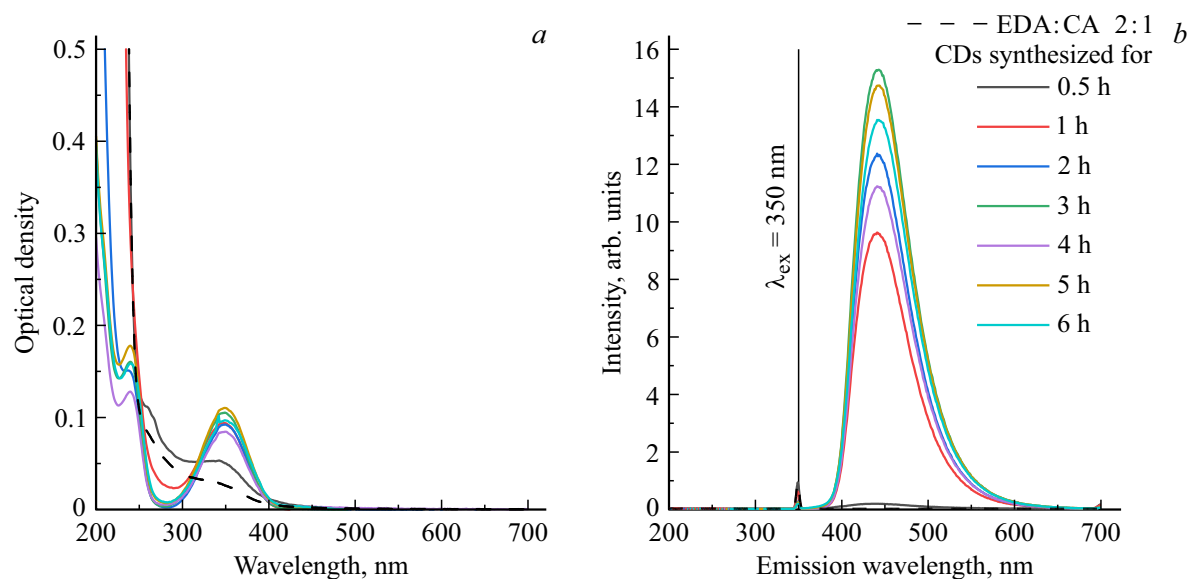


Figure 2. Optical density (a) and PL (b) spectra of the examined aqueous CD solutions.

examined without dilution, while the dilution ratio of other solutions was as high as 4001 (0.5 μL of the initial solution in 2000 μL of water; exact dilution ratios are listed in the Table 1). The optical density spectra and the corresponding PL spectra under excitation at wavelength λ_{ex} for diluted CD samples are shown in Fig. 2. PL QY values were calculated based on these spectra in accordance with the reference dye method; the obtained values are listed in the Table 1.

As one would expect, PL of CDs synthesized from EDA and CA (mixed in a 2:1 ratio) is related closely to their absorption. Notably, intense PL is observed when the CD absorption peak with a maximum around 350 nm becomes well-pronounced. If this peak is weak against the background of a broad shoulder of another absorption feature (this is largely true for CD 0.5 h and, in a lesser degree, for CD 1 h), the PL intensity and the corresponding QY values are far from their maxima. However, as the synthesis time increases (2–6 h), the absorption band with its maximum at 350 nm becomes better distinguished, the CD PL intensity under excitation at 350 nm increases, and the corresponding QY gets close to 100%. With the synthesis time kept within the indicated range, no significant changes were observed in the shape of both absorption and PL spectra.

IR absorption spectroscopy of CDs and precursors

IR absorption spectra of precursors and their mixture (Fig. 3) and all the synthesized CD samples (Fig. 4) were recorded in order to reveal the variation of CD structure in the process of synthesis.

It follows from Fig. 3 that the IR absorption spectrum of EDA features the bands of valence (3280–3360 cm^{-1}) and deformation (1600 cm^{-1}) vibrations of amino groups $-\text{NH}_2$ and the bands of valence (2800–2970 cm^{-1}), de-

formation (1460 cm^{-1}), and rotational (760–960 cm^{-1}) vibrations of methylene groups $-\text{CH}_2-$ [24]. The IR absorption spectrum of CA is dominated by the bands of valence (3000–3600 cm^{-1}) and deformation (1630 cm^{-1}) vibrations of $-\text{OH}$ groups and adsorbed water, the broad shoulder of valence O-H vibrations (2500–3400 cm^{-1}), and the bands of valence vibrations of C=O (1700 cm^{-1}) and C-O (1190–1210 cm^{-1}) of carboxyl groups $-\text{COOH}$ [25]. The results of comparative analysis of IR absorption spectra of individual precursors and their mixture (EDA:CA 2:1) in water suggest that precursors start reacting chemically prior to the onset of hydrothermal synthesis. The bands of carboxyl groups of CA and methyl and amino groups of EDA vanish in the mixture spectrum; the bands with maxima at 1540 and 1375 cm^{-1} become dominant (Fig. 3). It is likely that the indicated bands in the mixture spectrum are induced by valence symmetric (1375 cm^{-1}) and asymmetric (1540 cm^{-1}) vibrations of nitro group $-\text{NO}_2$ and valence vibrations of nitroso group $-\text{N}=\text{O}$ (1540 cm^{-1}) [26]. However, it should be noted that the product of reaction in a mixture of CA and EDA in water is a colorless liquid that features neither a pronounced absorption band with its maximum at 350 nm nor PL.

Figure 4 presents the IR absorption spectra of all the studied samples and the absorption spectrum of the precursor mixture prior to CD synthesis. The obtained data reveal that CD spectra undergo the following changes as the synthesis time increases from 0.5 to 6 h: the broad band of valence O-H vibrations at 2500–3500 cm^{-1} shifts toward higher wavenumbers; bands with maxima at 1647 cm^{-1} (valence vibrations of nonaromatic C=C bonds) and 1540, 1480, 1433, 1325, 1290, 1214, 1155, 1047, 775, and 585 cm^{-1} emerge and grow; the band of symmetric vibrations of nitro group $-\text{NO}_2$ at 1375 cm^{-1} vanishes, while two bands with maxima at 1390 and 1356 cm^{-1} emerge in its vicinity (all

Table 1. PL QY values of synthesized CDs at wavelength $\lambda_{\text{ex}} = 350$ nm and dilution ratios of CD solutions

Parameters	CDs prepared with different synthesis times						
	0.5 h	1 h	2 h	3 h	4 h	5 h	6 h
Synthesis time	0.5 h	1 h	2 h	3 h	4 h	5 h	6 h
QY*	15.1%	78.3%	97.8%	105.7%	85.4%	85.7%	97.9%
Dilution ratio used	—	5.7	1334	4001	4001	2301	2858

Note. * The statistical error of PL QY determination by the reference dye method is on the order of 10% of the obtained value.

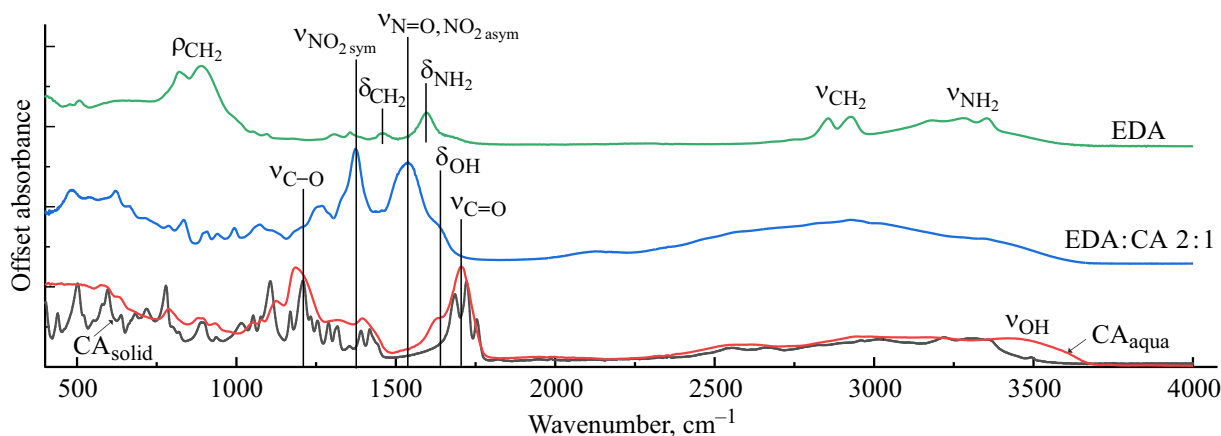


Figure 3. IR absorption spectra of CD precursors positioned on the FTIR crystal: liquid ethylenediamine (EDA), citric acid powder (CA_{solid}), and CA dried from aqueous solutions (CA_{aqua}). The spectrum of the used precursor mixture is designated as EDA:CA 2:1.

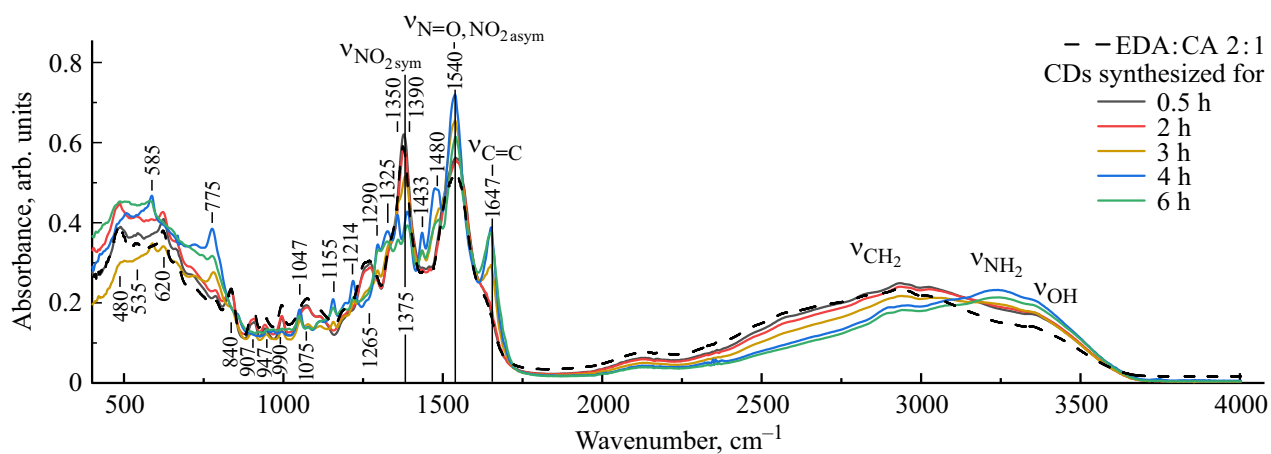


Figure 4. IR absorption spectra of the precursor mixture prior to hydrothermal synthesis and synthesized QDs dried from aqueous solutions on the FTIR crystal.

the mentioned bands are indicated above the plot in Fig. 4); and the bands with maxima at 1375, 1265, 1075, 990, 947, 907, 840, 620, 535, and 480 cm^{-1} (indicated below the plot in Fig. 4) weaken and vanish.

The mentioned IR absorption bands in the fingerprint region ($< 1500 \text{ cm}^{-1}$) may belong to different variants of both valence and deformation vibrations of C-O, C-H, C-N, and N-H groups in various environments; their unambiguous interpretation is a separate task that is beyond the scope of the present paper. The observed changes of interpretable absorption bands suggest that the process of CD synthesis

is, as expected, associated with carbonization of molecules. Since no absorption bands of aromatic carbon bonds are found in the IR absorption spectra of CDs measured in the process of synthesis and after it, one may conclude that the synthesized CDs have a copolymer structure and not an aromatic graphene one. This conclusion agrees with the results reported in [21]. Nitro groups $-\text{NO}_2$, which form when precursors are mixed, decompose in the process of synthesis, presumably triggering the formation of nitroso groups $-\text{N}=\text{O}$. Hydrogen bonds of water adsorbed on the nanoparticle surface and of surface O-H groups

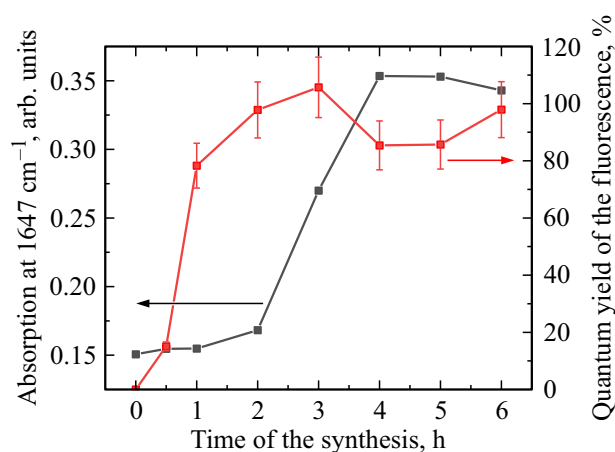


Figure 5. Dependences of the CD IR absorption intensity at 1647 cm^{-1} and the QY of CD PL on the hydrothermal synthesis time.

grow weaker: in parallel with molecule carbonization, polar properties of the CD surface become less pronounced (while hydrophobic properties grow in strength).

Interrelation between the changes in PL and CD structure

It is hard to evaluate quantitatively the changes in parameters of bands in IR absorption spectra of samples placed on the FTIR accessory, since these spectra cannot be normalized: the sample thickness may vary slightly, and the dryness factor (and, consequently, the intensity of broad water absorption bands) varies somewhat from one sample to the other. In view of this, the change in CD structure in the process of synthesis was characterized by the intensity of the band with its maximum at 1647 cm^{-1} that is associated with valence vibrations of nonaromatic C=C bonds and undergoes the greatest change. The chosen band is positioned at the shoulder of deformation OH vibrations, which is approximately the same for all CD samples (Fig. 4). The QY of CD PL at a wavelength of 350 nm was used as a quantitative characteristic of CD PL. Dependences of the intensity of the CD IR absorption band with its maximum at 1647 cm^{-1} and the QY of CD PL on the hydrothermal synthesis time were plotted (Fig. 5).

It follows from the obtained dependences (Fig. 5) that the intensity of the chosen band with its maximum at 1647 cm^{-1} remains almost unchanged in the spectra of the first three CD samples (0.5–2 h) and is close in magnitude to the intensity of the same band in the spectrum of a „sample“ with zero synthesis time (the initial EDA:CA 2:1 precursor mixture). The intensities of the 1647 cm^{-1} absorption band in the spectra of the three last CD samples (4–6 h) are also similar, but differ from those corresponding to the first three samples. Lying between these two groups, the central (fourth) sample synthesized within 3 h is the „transition“ one.

In the dependence of PL QY on the synthesis time, the „transition“ stage between samples with weak and strong PL corresponds to the interval between CD 0.5 h and CD 1 h: after just 2 h of synthesis, the QY reaches its maximum of $\sim 100\%$. The mismatch between „transition“ moments verifies the validity of the molecular model of PL of CDs synthesized from CA and EDA, which states that PL is induced by specific molecular luminophores attached to the carbon framework of CDs [19–21].

Thus, the results of comparison of IR absorption spectroscopy data with PL spectroscopy and optical absorption spectroscopy data suggest that three distinct stages of CD synthesis from EDA and CA may be identified.

1) Chemical transformations occur immediately after the mixing of precursors (citric acid and ethylenediamine) in water at room temperature: carboxyl groups of CA and amide groups of EDA decompose, and nitro and nitroso groups become dominant in IR absorption spectra (Fig. 3). The produced compounds feature no PL and no marked absorption bands in the UV optical region.

2) The synthesis of highly efficient luminophores starts 30 min after the onset of hydrothermal synthesis at a temperature of $140\text{ }^\circ\text{C}$ and reaches high rate levels in another 30 min. These luminophores have two excitation channels with centers at 242 and 350 nm, and their QY at $\lambda_{\text{ex}} = 350\text{ nm}$ is $\sim 100\%$. When the synthesis time reaches 2 h, the amount of such luminophores becomes sufficient for their absorption at 350 nm to become distinguishable (in other words, become dominant over the wing of another absorption). The QY of the CD solution as a whole then reaches $\sim 100\%$. It follows from the comparison of dependences of PL QY levels and the required dilution ratio of CD solutions on the synthesis time (see the Table 1) that the maximum amount of CD luminophores is synthesized within 3 h. However, the synthesis of these luminophores, which is seen clearly in PL and UV optical absorption spectra of CDs, leaves almost no trace in IR absorption spectra.

3) A synthesis time of 3 h is the threshold for changes in IR absorption spectra. When this threshold is crossed, the CD structure starts changing profoundly: molecule carbonization occurs, and these molecules form the copolymer carbon framework of synthesized CDs. Nitro groups- NO_2 , which formed when precursors were mixed, decompose in the process, providing building blocks for the formation of nitroso groups $-\text{N}=\text{O}$. This process reduces the number of surface polar groups of CDs and makes the hydrophobic properties of the nanoparticle surface more pronounced. The onset of CD framework carbonization does not alter the emissive efficiency of luminophores synthesized earlier. However, a fraction of molecular luminophores lose their fluorescence capacity in the course of subsequent synthesis (after 4 h); after 5 h of synthesis, their structure changes so profoundly that the absorption at 350 nm also vanishes (see the PL QY and the CD dilution ratio in the Table 1). These changes do not affect the emissive properties of remaining luminophores.

Conclusion

The structure and optical properties of CDs synthesized hydrothermally from a 2:1 mixture of EDA and CA at a temperature of 140 °C with the synthesis time varying within the 0.5–6 h range were examined. Three distinct stages of CD synthesis from EDA and CA were identified based on the results of IR absorption spectroscopy, PL spectroscopy, and optical absorption spectroscopy.

1) Chemical transformations of precursors at room temperature as a result of their mixing in water: carboxyl groups of CA and amide groups of EDA decompose, and nitro and nitroso groups form.

2) Synthesis of highly efficient luminophores with a QY on the order of 100% at $\lambda_{\text{ex}} = 350$ nm: these luminophores start to form after 30 min of reaction at a temperature of 140 °C, and their amount is maximized in 3 h.

3) Molecule carbonization and formation of the copolymer CD framework: the threshold reaction time is 3 h.

The CD PL intensity induced by highly efficient molecular luminophores increases with the amount of synthesized luminophores at stage 2 and may decrease at stage 3 due to their partial decomposition in the process of synthesis of the copolymer CD framework. The obtained data help refine the model of chemical transformations in the process of synthesis of ultrabright CDs from EDA and CA and confirm that they have a copolymer structure with molecular PL.

Acknowledgments

Certain experimental data used in this work were obtained using an IR Fourier spectrometer that was purchased under the Development Program of Moscow State University (agreement No. 65 dated October 04, 2021).

Funding

This study was supported by grant No. 23-72-01042 from the Russian Science Foundation (<https://rscf.ru/en/project/23-72-01042/>).

Conflict of interest

The authors declare that they have no conflict of interest.

References

- [1] D. Ozyurt, M.A. Kobaisi, R.K. Hocking, B. Fox. *Carbon Trends*, **12**, 100276 (2023). DOI: 10.1016/j.cartre.2023.100276
- [2] N.A.S. Omar, Y.W. Fen, R. Irmawati, H.S. Hashim, N.S.M. Ramdzan, N.I.M. Fauzi. *Nanomater.*, **12** (14), 2365 (2022). DOI: 10.3390/nano12142365
- [3] J. Liu, R. Li, B. Yang. *ACS Cent. Sci.*, **6** (12), 2179 (2020). DOI: 10.1021/acscentsci.0c01306
- [4] G. Bikbaeva, A. Pilip, A. Egorova, I. Kolesnikov, D. Pankin, K. Laptinskiy, A. Vervalde, T. Dolenko, G. Leuchs, A. Manzhina. *Nanomater.*, **13** (17), 2409 (2023). DOI: 10.3390/nano13172409
- [5] S. Wu, C. Zhou, C. Ma, Y. Yin, C. Sun. *J. Chem.*, **2022**, 1 (2022). DOI: 10.1155/2022/3737646
- [6] M.Yu. Khmeleva, K.A. Laptinskiy, P.S. Kasyanova, A.E. Tomskaya, T.A. Dolenko. *Opt. Spectrosc.*, **130** (6), 697 (2022). DOI: 10.21883/eos.2022.06.54706.36-22.
- [7] A.M. Vervalde, K.A. Laptinskiy, G.N. Chugreeva, S.A. Burikov, T.A. Dolenko. *J. Phys. Chem. C*, **127** (44), 21617 (2023). DOI: 10.1021/acs.jpcc.3c05231
- [8] Z. Zhu, H. Niu, R. Li, Z. Yang, J. Wang, X. Li, P. Pan, J. Liu, B. Zhou. *Biosens. Bioelectron.*: X, **10**, 100141 (2022). DOI: 10.1016/j.biosx.2022.100141
- [9] H. Lee, Y.-C. Su, H.-H. Tang, Y.-S. Lee, J.-Y. Lee, C.-C. Hu, T.-C. Chiu. *Nanomater.*, **11** (7), 1831 (2021). DOI: 10.3390/nano11071831
- [10] S.P. Thota, S.M. Thota, S. Srimadh Bhagavatham, K. Sai Manoj, V.S. Sai Muthukumar, S. Venkatesh, P.V. Vadlani, S.K. Belliraj. *IET Nanobiotechnol.*, **12** (2), 127 (2017). DOI: 10.1049/iet-nbt.2017.0038
- [11] H. Singh, A. Bamrah, M. Khatri, N. Bhardwaj. *Mater. Today: Proc.*, **28**, 1891 (2020). DOI: 10.1016/j.matpr.2020.05.297
- [12] N.A. Nazibudin, M.F. Zainuddin, C.A.C. Abdullah. *J. Adv. Res.*, **101** (1), 192 (2023). DOI: 10.37934/arfims.101.1.192206
- [13] Y. Dong, H. Pang, H.B. Yang, C. Guo, J. Shao, Y. Chi, C.M. Li, T.Yu. *Angew. Chem. Int. Ed.*, **52** (30), 7800 (2013). DOI: 10.1002/anie.201301114
- [14] T. Prathumsuwan, S. Jamnongsong, S. Sampattavanich, P. Paoprasert. *Opt. Mater.*, **86**, 517 (2018). DOI: 10.1016/j.optmat.2018.10.054
- [15] S. Mohapatra, M.K. Bera, R.K. Das. *Sens. Actuators B. Chem.*, **263**, 459 (2018). DOI: 10.1016/j.snb.2018.02.155
- [16] K.A. Laptinskiy, S.A. Burikov, S.V. Patsaeva, I.I. Vlasov, O.A. Shenderova, T.A. Dolenko. *Spectrochim. Acta A Mol. Biomol. Spectrosc.*, **229**, 117879 (2020). DOI: 10.1016/j.saa.2019.117879
- [17] J. Ren, L. Malfatti, P. Innocenzi. *C – J. Carbon Research*, **7** (1), 2 (2020). DOI: 10.3390/c7010002
- [18] D. Qu, M. Zheng, L. Zhang, H. Zhao, Z. Xie, X. Jing, R.E. Haddad, H. Fan, Z. Sun. *Sci. Rep.*, **4** (1), (2014). DOI: 10.1038/srep05294
- [19] J. Schneider, C.J. Reckmeier, Y. Xiong, M. von Seckendorff, A.S. Susha, P. Kasák, A.L. Rogach. *J. Phys. Chem. C*, **121** (3), 2014 (2017). DOI: 10.1021/acs.jpcc.6b12519
- [20] P. Duan, B. Zhi, L. Coburn, C.L. Haynes, K. Schmidt-Rohr. *Magn. Reson. Chem.*, **58** (11), 1130 (2020). DOI: 10.1002/mrc.4985
- [21] M. Zhang, X. Long, Y. Ma, S. Wu. *Opt. Mater.*, **135**, 113311 (2023). DOI: 10.1016/j.optmat.2022.113311
- [22] J.R. Lakowicz. *Principles of Fluorescence Spectroscopy* (Springer US, 2006). DOI: 10.1007/978-0-387-46312-4
- [23] Y. Zhang, R. Yuan, M. He, G. Hu, J. Jiang, T. Xu, L. Zhou, W. Chen, W. Xiang, X. Liang. *Nanoscale*, **9** (45), 17849 (2017). DOI: 10.1039/c7nr05363k
- [24] A.D. Allen, C.V. Senoff. *Can. J. Chem.*, **43** (4), 888 (1965). DOI: 10.1139/v65-115
- [25] L.C. Bichara, H.E. Lanús, E.G. Ferrer, M.B. Gramajo, S.A. Brandán. *Adv. Phys. Chem.*, **2011**, 1 (2011). DOI: 10.1155/2011/347072
- [26] *Infrared and Raman Characteristic Group Frequencies: Tables and Charts*. 3rd ed. by G. Socrates (The University of West London, U.K., 2001). DOI: 10.1021/ja0153520

Translated by D.Safin